

REFERENCES

1. Y. Hua, Estimating two-dimensional frequencies by matrix enhancement and matrix pencil, *IEEE Trans Signal Process* 40 (1992), 2267–2280.
2. S. Rouquette and M. Najim, Estimation of frequencies and damping factors by two-dimensional ESPRIT type methods, *IEEE Trans Signal Process* 49 (2001), 237–245.
3. L.C. Potter, D.M. Chiang, R. Carriere, and M.J. Gerry, GTD-based parametric model for radar scattering, *IEEE Trans Antennas Propag* 43 (1995), 1058–1067.
4. I.J. Gupta, High-resolution radar imaging using 2-D linear prediction, *IEEE Trans Antennas Propag* 42 (1994), 31–37.
5. J.W. Odendaal, E. Barnard, and C.W.I. Pistorius, Two-dimensional superresolution radar imaging using the MUSIC algorithm, *IEEE Trans Antennas Propag* 42 (1994), 1386–1391.
6. Y. Hua and T.K. Sarkar, On SVD for estimating generalized eigenvalues of singular matrix pencil in noise, *IEEE Trans Signal Process* 39 (1991).
7. Y. Hua, E. Baqai, Y. Zhu, and D. Heilbronn, Imaging of point scatterers from step-frequency ISAR data, *IEEE Trans Aerospace Electron Syst* 29 (1992), 195–205.
8. S. Rouquette and M. Najim, A new pairing step the MEMP method, *IEEE Conf Record of 31st ASILOMAR Conf Signal System Computer* 2 (1998), 1715–1719.
9. K.T. Kim, S.W. Kim, and H.T. Kim, Two-dimensional ISAR imaging using full polarization and super resolution processing techniques, *IEE Proc Radar Sonar Navign* 145 (1998).

© 2008 Wiley Periodicals, Inc.

INVESTIGATION OF BROADBAND POWER AMPLIFIER WITH HIGH POWER-COMBINING EFFICIENCY

Kaijun Song,^{1,2} Yong Fan,¹ and Xiaobing Zhou²

¹ School of Electronic Engineering, University of Electronic Science and Technology of China, Chengdu 610054, China; Corresponding author: ksong@mtech.edu

² Department of Geophysical Engineering, Montana Tech of the University of Montana, Butte, MT 59701

Received 23 December 2007

ABSTRACT: A four-device broadband solid-state power amplifier, which is based on radial waveguide power-dividing/combining circuit, has been investigated in this work. The fabricated power amplifier combining four monolithic microwave integrated circuit power amplifiers shows a 12–16.6 dB small-signal gain over a broadband from 6 to 14 GHz. The measured maximum output power at 1 dB compression is 25.6 dBm at 10 GHz, with a high power-combining efficiency of 96%. © 2008 Wiley Periodicals, Inc. *Microwave Opt Technol Lett* 50: 2178–2181, 2008; Published online in Wiley InterScience (www.interscience.wiley.com). DOI 10.1002/mop.23614

Key words: broadband; power amplifier; power-combining efficiency; radial waveguide

1. INTRODUCTION

Broadband solid-state power amplifiers with high power and high efficiency are of interest in many applications such as UWB system, satellite communication system, commercial communications, and radar transmitter. Many researches in broadband high-efficiency amplifiers have been demonstrated by combining output powers from a number of solid-state devices at microwave and millimeter-wave frequencies [1–3]. Many broadband power-combining techniques have been proposed for the design of broadband

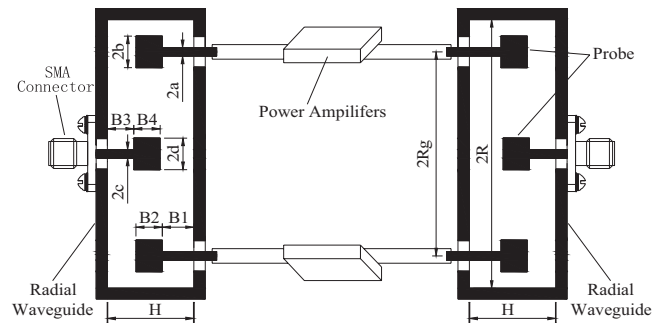


Figure 1 Topology of the radial waveguide power combiner

high-power microwave and millimeter-wave solid-state amplifiers [4–7]. Among various combiners, radial waveguide spatial power combiners are of practical interest because they do not suffer from spill-over losses and have high power-combining efficiency.

In a previous study, a broadband radial waveguide power divider using coaxial probe array that achieved low-loss waveguide-to-coaxial probe transitions has been designed and then simulated based on equivalent circuits by the authors [7]. By appropriate placement of coaxial probes in the radial waveguide, equal power distribution can be achieved. Experiments on the radial power divider have demonstrated its broadband characteristics.

In this work, a broadband power amplifier with high power-combining efficiency has been developed to demonstrate the applicability of the radial power divider/combiner at microwave frequencies. The fabricated power amplifier showed an output power of 25.6 dBm at 10 GHz, which indicates a maximum power-combining efficiency of 96% for the power combining amplifier. These topologies allow for broadband, low loss, good heat sinking capability, and ease of fabrication and have potential to meet the increasing demand of microwave and millimeter-wave communications and radar systems.

2. ANALYSIS AND DESIGN OF THE POWER DIVIDER

The structure of the radial waveguide power-combining circuit is shown in Figure 1. It consists of a divider and a combiner. Power is coupled to (or from) probe arrays placed in waveguides. RF power is input from the central probe of the left radial waveguide and then is divided four ways using four equispaced identical peripheral probes in the left radial waveguide. A short wall placed beyond the probe presents an open circuit to the probe. Each of the peripheral probes in the left radial waveguide couples the power from the radial waveguide and then feeds to the input port of a power amplifier. The amplified powers are then combined in the right radial waveguide using the right peripheral probe array. Finally, the combined power is output from the right central probe. Excitation of the power-dividing/combining circuits is accomplished by using TEM mode of a radial waveguide.

Figure 2 shows a simple model for the radial divider, where $\Phi_1 = k(R_g - R_o)$ and $\Phi_2 = k(R - R_g)$. A coaxial probe array in a radial waveguide is used to implement power dividing function. The circle of radius R_o is the reference plane, which divides the radial power-dividing structure into two volumes: a central cylindrical volume of radius R_o comprising the central probe and a cavity region (comprising the peripheral probes) outside the central cylindrical volume. The power divider can be viewed as a structure composed of four identical sectoral waveguides separated by magnetic side walls due to the symmetry.

According to the transmission-line approach, a two-port circuit can be used to model the central cylindrical volume comprising the

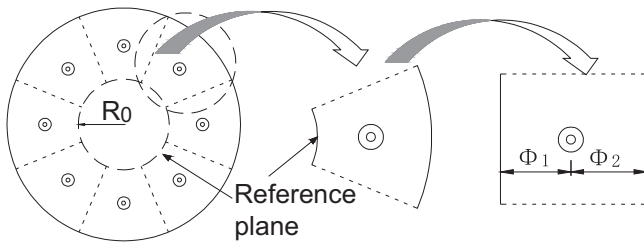


Figure 2 Schematic illustration of simple electromagnetic modeling

central probe, as shown in Figure 3. Figure 3(b) shows its equivalent circuit. $Y_c = G_c + jB_c$ is the central probe admittance, which can be determined according to [8], and i is the current source. The equivalent circuit of the radial line with a length $R_0 - d$ between reference radius R_0 and d may be schematically represented as the π -circuit shown in Figure 3 [9]. The shunt and series parameters of the π -circuit representation for the radial line are seen to be

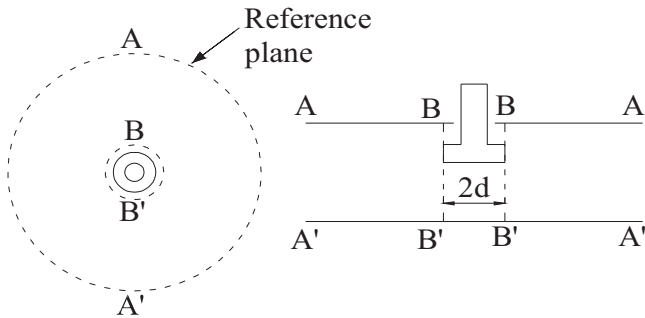
$$Y_{11} - Y_{12} = -jY_0(b) \left[ct(x,y) + \sqrt{\frac{y}{x}} ct(x,y) \right], \quad (1)$$

$$Y_{22} - Y_{12} = -jY_0(R_0) \left[-ct(y,x) + \sqrt{\frac{x}{y}} ct(y,x) \right], \quad (2)$$

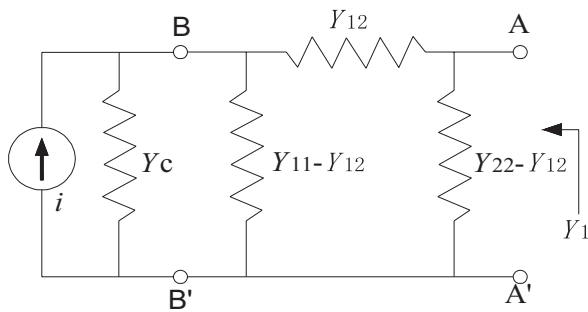
$$Y_{12} = -j\sqrt{Y_0(b)Y_0(R_0)} ct(x,y), \quad (3)$$

where

$$ct(x,y) = \sqrt{\frac{1 + ct(x,y)Ct(x,y)}{\xi(x,y)}},$$



(a)



(b)

Figure 3 Equationivalent circuit of the central cylindrical volume

Table 1 Dimensions of Radial Combiner (unit: mm)

a	b	c	d	R	R_g
0.65	1.5	0.65	1.5	10.5	7
B1	B2	B3	B4	H	
1.2	4.6	1.2	4.3	8.5	

$$ct(x,y) = \frac{J_1 N_{00} - N_1 J_{00}}{J_0 N_{00} - N_0 J_{00}},$$

$$Ct(x,y) = \frac{J_{10} N_0 - N_{10} J_0}{J_1 N_{10} - N_1 J_{10}},$$

$$\xi(x,y) = \frac{J_0 N_{00} - N_0 J_{00}}{J_1 N_{10} - N_1 J_{10}},$$

and

$$J_0(kb) = J_0, J_0(kR_0) = J_{00}, J_1(kR_0) = J_{10}, N_0(kb) = N_0, N_0(kR_0) = N_{00}, N_1(kR_0) = N_{10}, x = kb, y = kR_0, k = 2\pi/\lambda.$$

Then the admittance Y_1 seen from the right port [as shown in Fig. 3(b)] can be determined according to Eqs. (1)–(3) and the central probe admittance Y_c . Furthermore, the admittance of the sectoral waveguide comprising a peripheral probe, looking from reference plane to the short wall, is

$$Y_m = Y_p - j \cot(\Phi_2), \quad (4)$$

where $Y_p = G + jB$ is the admittance of a peripheral probe.

Therefore, if Φ_1 is chosen to be 0° at the designed frequency, design formulas for perfect power dividing are given as

$$Y_1 = 8Y_m = 8(Y_p - j \cot(\Phi_2)). \quad (5)$$

When the values of Y_c and Φ_2 are specified, those of the admittance Y_p can be determined to realize broadband matching, and then the peripheral probe dimensions can also be obtained according to [8]. From the analysis above, it is noted that the operation frequency and bandwidth are mainly determined by the probe dimensions and the electrical length between the waveguide short wall and the center of probe array. This structure can provide



Figure 4 Passive radial combiner

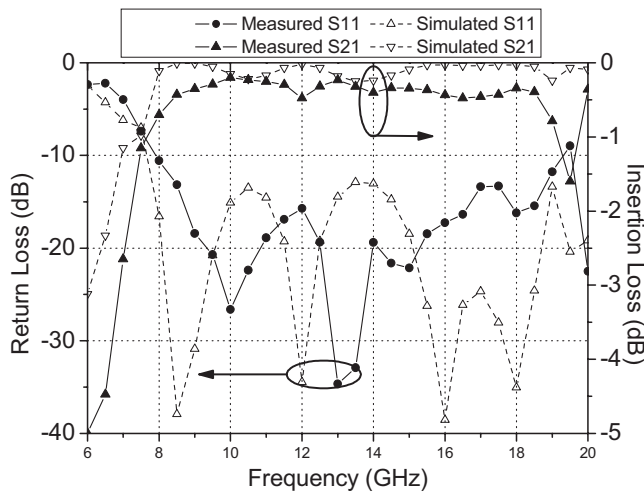


Figure 5 Simulated and measured results for the passive combiner

uniform illumination of the array and can be designed for wide-band operation.

3. DESIGN OF A FOUR-WAY PASSIVE RADIAL COMBINER

Based on the topology of the radial waveguide power combiner shown in Figure 1, a four-way passive radial combiner was designed. The power-dividing structure was simulated using Ansoft-HFSS. Dielectric and conductor losses were included in the simulation. The optimized dimensions of the radial waveguide, central coaxial probe, and peripheral coaxial probe are listed in Table 1. A passive radial combiner was built through machining of a waveguide cavity in the aluminum blocks by placing two identical power dividing circuits back to back, as shown in Figure 4. The coaxial probes have been inserted inside of the waveguide at the designed locations.

Figure 5 shows the measured and simulated insertion and return losses for the passive combiner. The measured results included the influences of the SMA connectors at input and output ports. The measured minimum insertion loss of the entire passive system is 0.2 dB at 10 GHz. The measured and simulated 10 dB return loss bandwidths were found to be ~81% and 91%, respectively. The bandwidth around which the minimum insertion loss increases by 0.5 dB was found to be 84.6% experimentally. Simulation predicted this value to be greater than 91%. Compared with the simulated results, the increased insertion loss is most likely attributed to the fabrication errors such as inaccuracies in assembling the coaxial probes and SMA connectors. Nevertheless, the simulated results show a good agreement with the measured response.

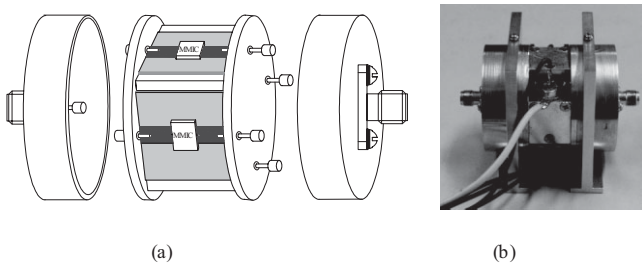


Figure 6 (a) Assembly of the radial waveguide power amplifier and (b) photograph of the radial waveguide power amplifier

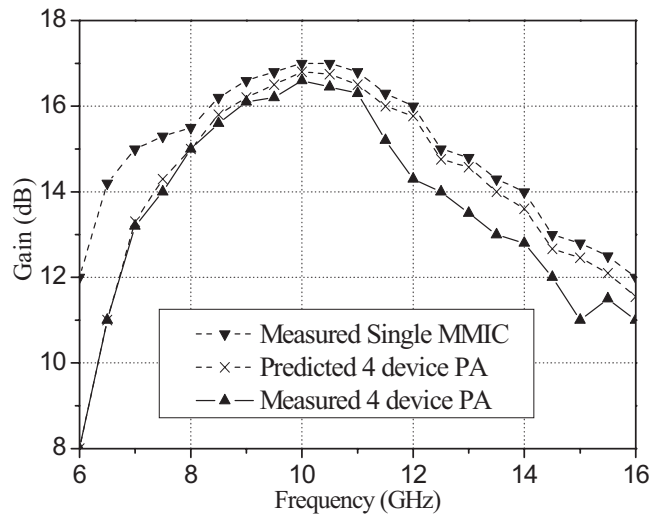


Figure 7 Predicted and measured small-signal gain

4. EXPERIMENTAL

Based on the passive combining system, a four-device power amplifier using Hittite HMC441LM1 power amplifiers was designed and fabricated. Efficient heat sinking of the power amplifiers was achieved by mounting the devices on the ground plane between two radial waveguides, as shown in Figure 6(a). The photograph of a radial waveguide power amplifier is shown in Figure 6(b).

A single MMIC amplifier was also fabricated to characterize its small- and large-signal response over the frequency range of interest (6–16 GHz). The individual HMC441LM1 showed a small-signal gain of 17 dB and an output power of 19.8 dBm at 10 GHz (see Fig. 7). Based on the measured single MMIC frequency response and simulation results of the passive radial-waveguide combiner, the small-signal response of the four-device power amplifier can be predicted. The predicted and measured small-signal gains of the four-device power amplifier roughly agree with each other, as shown in Figure 7. The power combining amplifier has 12–16.6 dB gain over a wide bandwidth from 6 to 14 GHz. The upper end bandwidth of the combiner is limited by the MMIC. The combiner itself has a potential to work up to 19 GHz, as shown in

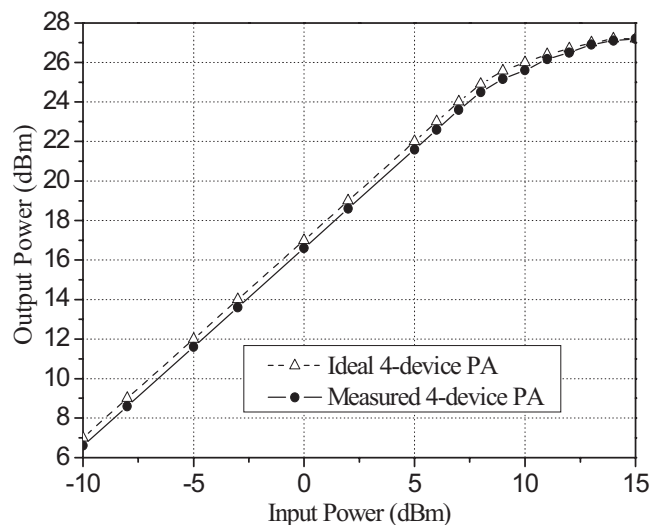


Figure 8 Output power of four device power amplifier at 10 GHz

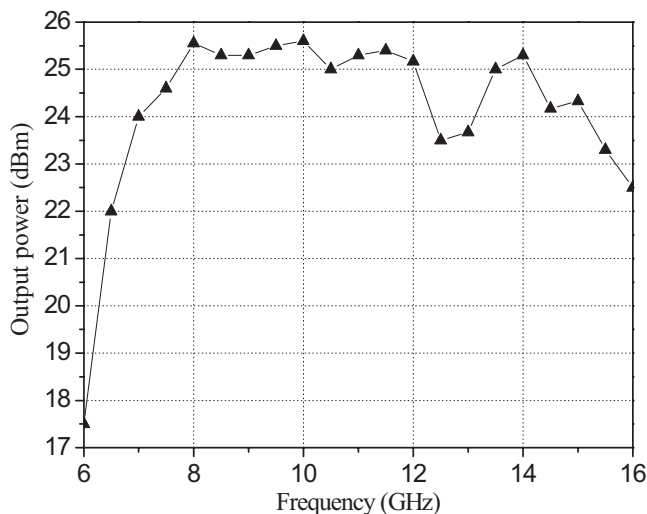


Figure 9 Measured Pout@1 dB of the four-device power amplifier

Figure 5. As mentioned earlier, the differences between simulation and measurement results are mainly attributed to the mechanical errors introduced in fabrication of the waveguide divider/combiner. It should also be noticed that the single MMIC amplifier's gain variation with frequency affects the overall power amplifier's gain flatness (see Fig. 7).

In addition, the power compression for the amplifier has been measured. The maximum output power at 1 dB gain compression has been achieved at 10 GHz with a value of 25.6 dBm [see Fig. 8]. The MMICs are biased at 5 V with a total DC current of 0.39 A. The overall power-added efficiency is $\sim 18.5\%$ at 10 GHz. The output power of the four-device power amplifier as a function of frequency is also shown in Figure 9.

Based on the measured insertion loss (S21) of the passive divider/combiner, the power-combining efficiency of the four-device amplifier can be calculated directly [10]. The power-combining efficiency of the four-way divider/combiner as a function of frequency is shown in Figure 10. The maximum power-combining efficiency was $\sim 96\%$ at 10 GHz.

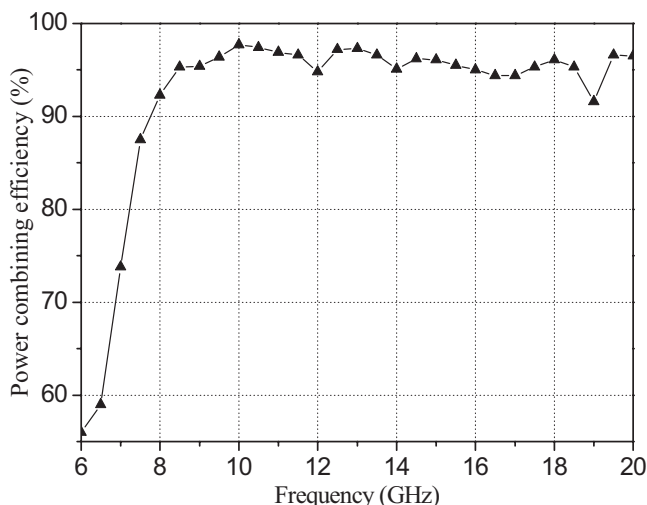


Figure 10 Power combining efficiency for the four-way power-dividing/combining circuit

5. CONCLUSION

A broadband power amplifier using radial waveguide power combining circuits has been designed and fabricated. The four-way passive radial combining circuit shows a minimum insertion loss of 0.2 dB at 10 GHz with an 11 GHz 0.5 dB bandwidth. The active circuit demonstrates a maximum small-signal gain of 16.6 dB at 10 GHz with a 3 dB bandwidth of 6 GHz. The output power of the four-device power amplifier as a function of frequency is also measured. The maximum output power at 1 dB gain compression has been achieved with a value of 25.6 dBm at 10 GHz, corresponding to a high power-combining efficiency of 96%. This technique has the potential to be applied to millimeter-wave communications and radar system.

REFERENCES

1. P.C. Jia, L.-Y. Chen, and A. Alexanian, "Broad-band high-power amplifier using spatial power-combining technique," *IEEE Trans Microwave Theory Tech* 51 (2003), 2469–2475.
2. X. Jiang, S.C. Ortiz, A. Mortazawi, "A Ka-band power amplifier based on the traveling-wave power-dividing/combining slotted-waveguide circuit," *IEEE Trans Microwave Theory Tech* 52 (2004), 633–639.
3. N.S. Cheng, T.P. Dao, M.G. Case, D.B. Rensch, and R.A. York, "A 120-watt X-band spatially combined solid state amplifier," *IEEE Trans Microwave Theory Tech* 47 (1999), 2557–2561.
4. K. Song, Y. Fan, and Y. Zhang, "A microstrip probe coaxial waveguide power divider/combiner," *Int J Infrared Millimet Waves* 27 (2006), 1269–1279.
5. A. Alexanian and R.A. York, "Broadband waveguide-based spatial combiner," *IEEE MTT-S Int Microwave Symp Dig* 3 (1997), 1139–1142.
6. K. Song, Y. Fan, and Y. Zhang, "Investigation of a power divider using a coaxial probe array in a coaxial waveguide," *IEE Proc Microwave Antennas Propag* 1 (2007), 900–903.
7. K. Song, Y. Fan, Y. Zhang, "Broad-band power divider based on radial waveguide," *Microwave Opt Tech Lett* 49 (2007), 595–597.
8. M.E. Bialkowski, "Analysis of disc-type resonator mounts in parallel plate and rectangular waveguides," *Arch Elektron Uebertragungstechnik AEU* 38 (1984), 306–311.
9. N. Marcuvitz, "Waveguide handbook," McGraw-Hill, New York, 1951, pp. 42–53.
10. M.S. Gupta, "Power combining efficiency and its optimization," *IEE Proc Microwave Antennas Propag* 139 (1992), 233–238.

© 2008 Wiley Periodicals, Inc.

WIDE-SLOT WAVEGUIDE ANTENNA ON LTCC TECHNOLOGY

B. L. Ooi,¹ Irene Ang,¹ X. C. Shan,² Albert Lu,² R. Fieck,³ and H. D. Hristov³

¹ Department of Electrical and Computer Engineering, National University of Singapore, 10 Kent Ridge Crescent, Singapore 119260; Corresponding author: eleooibl@nus.edu.sg

² Singapore Institute of Manufacturing Technology, Singapore

³ Departamento de Electronica, Universidad Tecnica Federico Santa Maria, Valparaiso, Chile

Received 24 December 2007

ABSTRACT: A wide-slot waveguide antenna implemented on low-temperature cofired ceramic technology is presented. The overall antenna is excited by aperture coupling. The design is simulated and validated by experimental measurement. The measured result shows that a 10-dB return loss has been achieved across the bandwidth from 2.6 GHz to 12.8 GHz, thus amounting to 132.5%. The measured radiation pattern of the proposed antenna is also presented and discussed. © 2008 Wiley Periodicals, Inc. *Microwave Opt Technol Lett* 50: 2181–2184, 2008;